Available online at www.sciencedirect.com

ScienceDirect

Procedia Structural Integrity 28 (2020) 472–481

Structural Integrity Procedia

www.elsevier.com/locate/procedia

1st Virtual European Conference on Fracture

Investigation of the effect of porosity on intergranular brittle fracture using peridynamics

Mingyang Li[a,*], Selda Oterkus[a], Erkan Oterkus[a]

[a]*PeriDynamics Research Centre, Department of Naval Architecture, Ocean and Marine Engineering, University of Strathclyde, 100 Montrose Street, Glasgow G4 0LZ, UK*

Abstract

Brittle materials are widely used and their fracture behaviour can be significantly influenced by their microstructures and microstructural defects including pores, microcracks, grains and grain boundaries. In this study, the effect of porosity on intergranular fracture behaviour of polycrystalline materials is investigated by using peridynamics. Different number of cases are considered for different number of grains, different porosity ratios, different locations of pores and different grain boundary strengths. It is concluded that the severity of the cracks, especially the newly created cracks, are influenced by the number of grains and porosity. Moreover, with the increase of grain boundary strength, the effect of porosity dramatically decreases and the fracture pattern in microscale becomes identical to the macroscale crack pattern.

Keywords: Peridynamics; Polycrystal; Porosity; Brittle; Intergranular

1. Introduction

Brittle materials are widely used and their fracture behaviour can be significantly influenced by their microstructures and microstructural defects including pores, microcracks, grains and grain boundaries. In this study, the effect of porosity on intergranular fracture behavior of polycrystalline materials is investigated by using

* Corresponding author. Tel.: +44-141-548-3876.
E-mail address: m.li@strath.ac.uk

2452-3216
10.1016/j.prostr.2020.10.056

peridynamics. Peridynamics (PD) is a non-local continuum mechanics formulation introduced by Silling (2000). PD is very suitable for failure prediction in materials and structures. It can be applicable at all scales ranging from macro-scale to micro-scale. There has been a rapid progress on peridynamics especially during the recent years. Application of PD theory is not limited to metals (Oterkus et. al. 2010b), but can be used for other materials such as composites (Oterkus et. al., 2010a; Oterkus and Madenci, 2012a,b), concrete (Oterkus et. al., 2012) and graphene (Liu et. al., 2018). There are several PD formulations available for simplified structures including Euler beam (Diyaroglu et. al., 2019), Kirchhoff plate (Yang et. al., 2020), Timoshenko beam (Diyaroglu et. al., 2015) and Mindlin plate (Vazic et. al., 2020). It is possible to implement peridynamic beam and plate formulations in commercial finite element packages (Yang et. al., 2019). PD theory was utilized for topology optimization of cracked structures by Kefal et. al. (2019). Vazic et. al. (2017) and Basoglu et. al. (2019) used PD theory to study the effect of microcracks on the propagation of a macrocrack. Imachi et. al. (2019) developed a new transition bond approach for failure definition which was applied for dynamic fracture analysis including crack arrest (Imachi et. al., 2020). PD theory has been extended to other physical fields including thermal diffusion (Oterkus et. al., 2014), moisture diffusion (Diyaroglu et. al., 2017a,b), lithiation (Wang et. al., 2018) and pitting corrosion (De Meo et. al., 2017). An extensive review on peridynamics can be found in Madenci and Oterkus (2014) and Javili et. al. (2019).

There are currently available peridynamic formulations to model polycrystalline materials (De Meo et. al., 2016; De Meo et. al., 2017; Zhu et. al., 2016; Li et. al., 2020; Lu et. al., 2020) and different properties can be specified to both individual grains and grain boundaries. Therefore, it is possible to capture both intergranular and transgranular fracture modes. In this study, the porosity at the grain boundaries will be explicitly modelled by using peridynamics to determine the effect of porosity on the intergranular fracture of polycrystalline materials for the first time in the literature.

2. Peridynamic model for polycrystalline materials

PD theory is a non-local continuum mechanics formulation and its equation of motion can be expressed as

$$\rho(\mathbf{x})\ddot{\mathbf{u}}(\mathbf{x},t)=\int_{H_{\mathbf{x}}}\mathbf{f}\left(\mathbf{u}(\mathbf{x}',t)-\mathbf{u}(\mathbf{x},t),\mathbf{x}'-\mathbf{x}\right)dV_{\mathbf{x}'}+\mathbf{b}(\mathbf{x},t) \tag{1}$$

where $\rho(\mathbf{x})$ is the density, $\mathbf{u}(\mathbf{x},t)$ and $\ddot{\mathbf{u}}(\mathbf{x},t)$ are the displacement and acceleration of the material point located at $\mathbf{x}$, $\mathbf{f}\left(\mathbf{u}(\mathbf{x}',t)-\mathbf{u}(\mathbf{x},t),\mathbf{x}'-\mathbf{x}\right)$ is peridynamic bond force between material points located at $\mathbf{x}$ and $\mathbf{x}'$, $\mathbf{b}(\mathbf{x},t)$ is the body load, t is time and $H_{\mathbf{x}}$ is the horizon, which is the domain of influence. In order to solve Eq. (1) numerically, Eq. (1) can be written in discrete form for the material point $\mathbf{x}_i$ as

$$\rho(\mathbf{x}_i)\ddot{\mathbf{u}}(\mathbf{x}_i,t)=\sum_{j=1}^{N}\mathbf{f}\left(\mathbf{u}(\mathbf{x}_j,t)-\mathbf{u}(\mathbf{x}_i,t),\mathbf{x}_j-\mathbf{x}_i\right)V_j+\mathbf{b}(\mathbf{x}_i,t) \tag{2}$$

where N is the number of material points inside the horizon and V_j is the volume of the material point j. The peridynamic bond force between two interacting material points $\mathbf{x}_i$ and $\mathbf{x}_j$ is defined as

$$\mathbf{f}=cs\frac{\mathbf{y}_j-\mathbf{y}_i}{\left|\mathbf{y}_j-\mathbf{y}_i\right|} \tag{3}$$

where c is the bond constant, s is the stretch, and $\mathbf{y}$ is the position of the material point in the deformed configuration. The stretch can be defined as

$$s = \frac{\left|\mathbf{y}_j - \mathbf{y}_i\right| - \left|\mathbf{x}_j - \mathbf{x}_i\right|}{\left|\mathbf{x}_j - \mathbf{x}_i\right|} \tag{4}$$

If the stretch exceeds a critical stretch value, s_0, then the bond is broken.

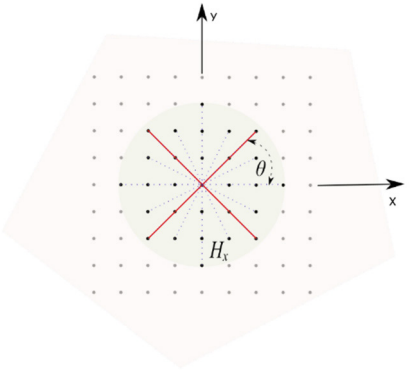

Fig. 1. PD model for a polycrystalline material when the orientation of the crystal is 0° (Li et. al., 2020).

As shown in Fig. 1, there are two different bond constants that are used to represent cubic crystals, which are considered in this study. Bonds represented by dashed lines, c_d, are in all directions whereas bonds represented by solid lines, c_s, are in particular directions with an angle of $\frac{\pi}{4}(2\times i-1), (i = 1, 2, 3, 4)$ with respect crystal orientation. Bond constants for these two types of bonds can be expressed in terms of components of the stiffness matrix of a cubic crystal, c_{11} and c_{12}, as

$$c_d = \frac{12\left(c_{11}{}^2 - c_{11}c_{12}\right)}{\pi h\delta^3 c_{11}} \tag{5a}$$

$$c_s = \frac{4\left(3c_{11}c_{12} - 2c_{12}{}^2 - c_{11}{}^2\right)}{\beta c_{11}} \tag{5b}$$

where $\beta = \sum_{j=1}^{N} \xi_{ij} V_j$, ξ_{ij} is the bond length between material points i and j, and δ is the horizon size.

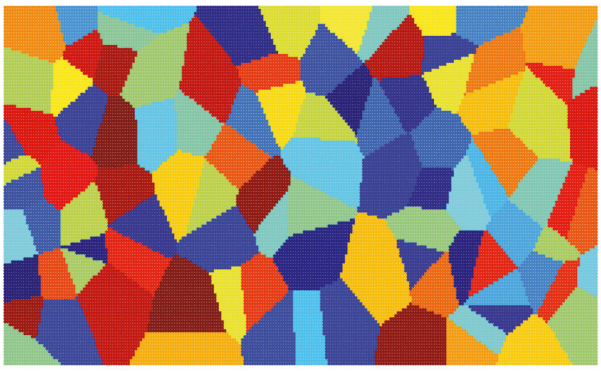

Fig. 2. Randomly generated polycrystals (Li et. al., 2020).

In order to generate the polycrystalline material model, Voronoi tessellation method is used (see Fig. 2). Grain sizes and orientations are randomly generated. The bond constants of the bonds crossing the grain boundaries are specified as the average of the bond constants of the interacting material points. Grain boundary coefficient (GBC) is defined as the ratio of the critical stretch of the grain boundary bonds and grain interior bonds.

3. Numerical results

In order to study the effect of porosity on the fracture of polycrystals, the polycrystalline material model considered in De Meo et. al. (2016) was utilized. The plate has a size of 5 mm $\times$ 5 mm and the thickness of the plate is 0.5 mm. The plate is made of AISI 4340 steel with material properties of $c_{11} = 208.9$ GPa and $c_{12} = 126.4$ GPa (Rimoli, 2009). There are two initial cracks defined at the top and bottom edges of the plate with a length of 0.4 mm and are located along the vertical central-line of the plate. For the basic PD parameters, there are 150×150 PD points and the grid distance is decided as $dx = 0.0333$ mm. Based on the suggestion provided in Madenci and Oterkus (2014), the horizon size of the analysis is fixed as $\delta = 3dx$. The critical stretch is specified as $s_0 = 0.0328$. A velocity boundary condition of 25 m/s was applied at the right and left boundaries of the plate by defining additional three layers of PD points (Fig. 3). The total number of the times steps is 2000 with a time step size of 1 ns. The variables of the analysis are the number of grains (crystals) and their distribution, the number of the pores and their distribution, and grain boundary strength. It should be mentioned that the grain boundary strength is represented by grain boundary coefficient (GBC). The GBC value is kept as 0.5 except the final case.

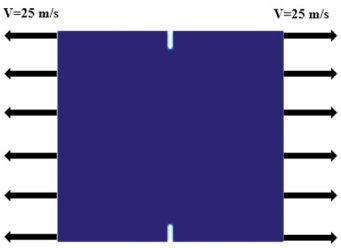

Fig. 3. The polcrystalline material model subjected to velocity boundary conditions.

In the first case, the results are provided for the plate with 150 grains without porosity as shown in Fig. 4. From the plots, it can be seen that the crack propagates through the grain boundaries from the pre-existing cracks to form the major crack. The majority of the cracks concentrate around the central region of the plate.

Fig. 4. Results of crack propagation without porosity at 2 μs; (a) crack distribution with grains, (b) damage.

Then, the porosity was introduced by creating randomly distributed small circles around the grain boundaries (Chakraborty et. al., 2016). The total number of the pores is 16 and each has a diameter of 0.2 mm. Eventually, the porosity ratio reaches approximately 2%. The distribution of the pores and the propagation of the crack with grains are shown in Fig. 5. The plots of the damage at 4 different time steps are also provided to give a more clear illustration of the fracture behaviour as the time progresses.

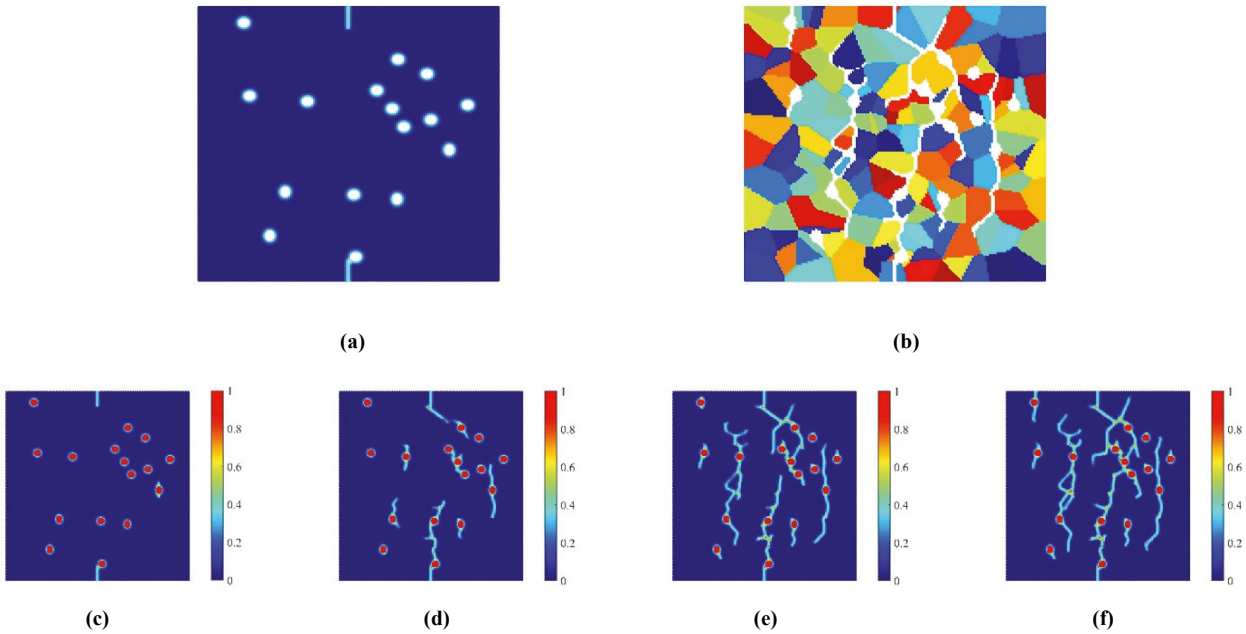

Fig. 5. The case with 150 grains and 2% porosity; (a) the distribution of pores, (b) crack distribution with 150 grains, (c) damage at 0.5 μs, (d) damage at 1 μs, (e) damage at 1.5 μs, (f) damage at 2 μs.

Compared to the without porosity case, for the main crack, it still propagates towards the opposite edge. However, there is a tendency for the main crack to propagate towards the pores, i.e. the propagation of the main crack has been appealed by the pores, especially those pores around the central region. Moreover, the branches of the main crack are slightly reduced at the same time. Additionally, there are small cracks that initiate from the pores and the direction of the propagation of these cracks is perpendicular to the loading direction. These small cracks propagate along the grain boundary to form newly generated branches of crack. Last but not least, the more intensive the pores, the more serious the new initiated cracks.

Another numerical case includes same grain distribution, but different locations of the pores to further support the former observations (Fig. 6). All of the previously mentioned features can still be captured as expected. Furthermore, an extra case with both different distributions of grains and pores is given to explore their effects. As shown in Fig. 7, crack behaviours are not significantly influenced by the distribution of grains or pores. From what has been shown, it can be concluded that porosity causes initiation of small cracks which propagate perpendicular to the loading direction to form new branches of crack. If the pores are intensive, this phenomenon becomes more obvious. These observations agree with the conclusions drawn by Chakraborty et al. (2016). The propagation of the major crack has also been changed. It prefers to propagate towards the pores and the branches have also been reduced. More importantly, grain distribution or pore distribution does not have a big impact on these observations.

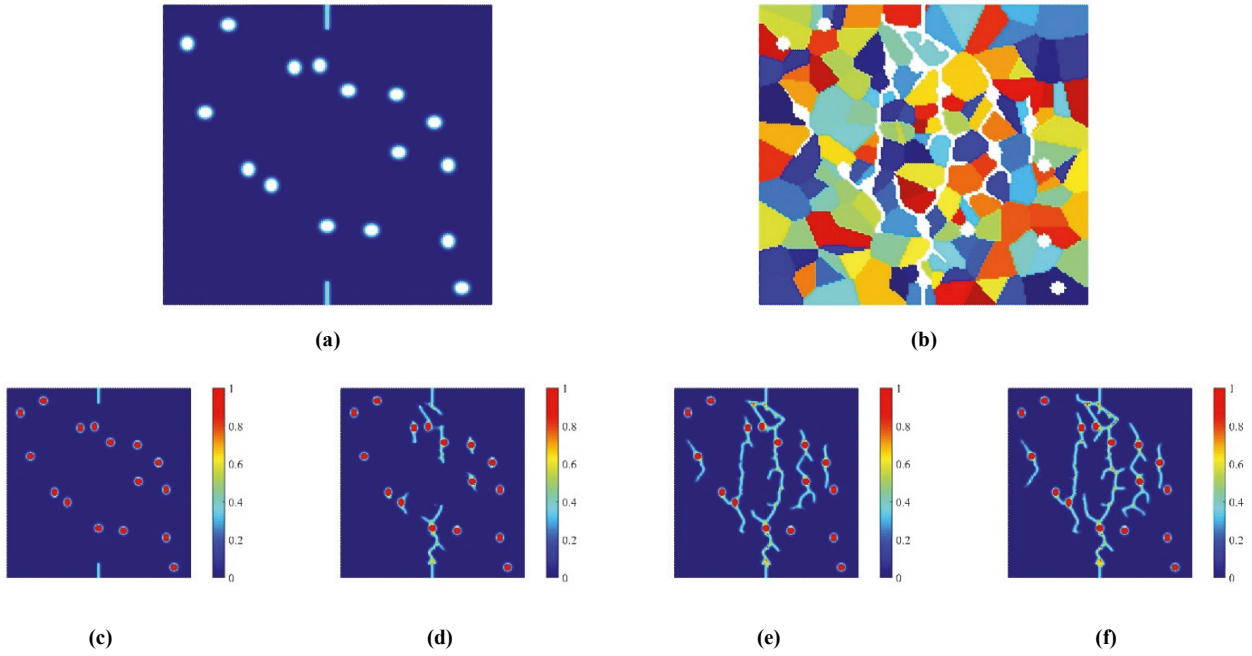

Fig. 6. The case with 150 grains but different 2% porosity distribution; (a) the distribution of pores, (b) crack distribution with 150 grains, (c) damage at 0.5 μs, (d) damage at 1 μs, (e) damage at 1.5 μs, (f) damage at 2 μs.

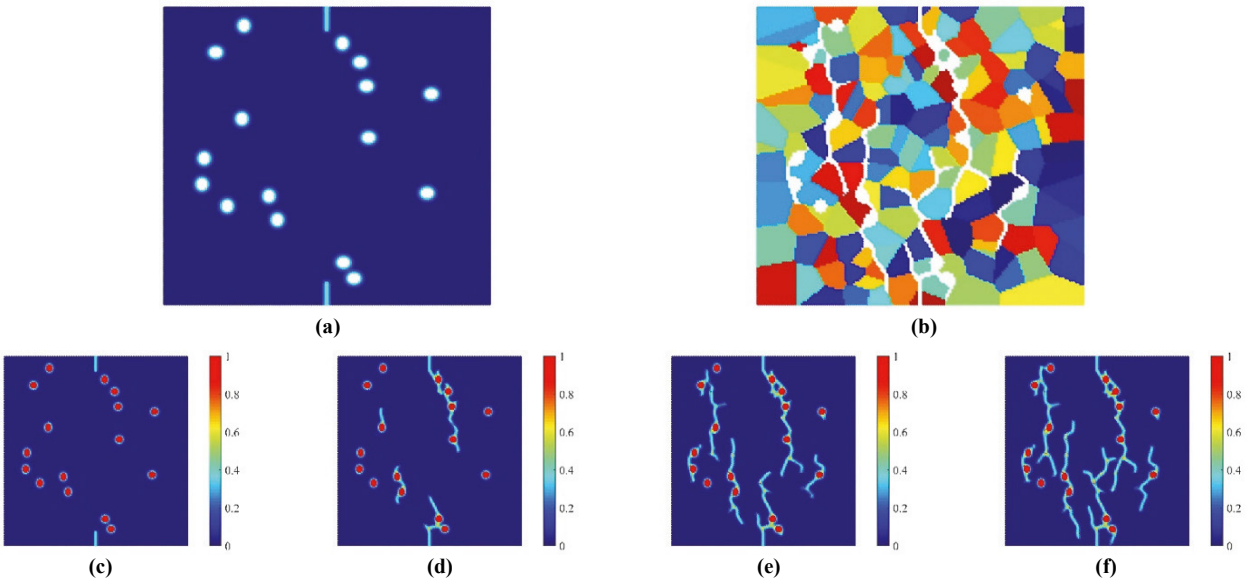

Fig. 7. The case with both different grain distribution and 2% porosity, (a) the distribution of pores, (b) crack distribution with 150 grains, (c) damage at 0.5 μs, (d) damage at 1 μs, (e) damage at 1.5 μs, (f) damage at 2 μs.

Additional three cases are considered to explore the effects of number of grains, porosity distribution, and the grain boundary strength. First of all, the number of grains is reduced from 150 to 100 and then to 50. The plots of the results are presented as Fig. 8. When the grain number is 100, although the severity of the fracture is decreased, the change

is not obvious. However, when it comes to 50 grains, only the characteristics of the major crack is dominant. Next, the grain number is constrained as 150, but the porosity ratio is increased from 2% to 5%, by rising 1% for each case (Fig. 9). Although the change is not obvious initially, with the rise of the porosity ratio, the severity of the fracture especially the main crack becomes increasingly significant.

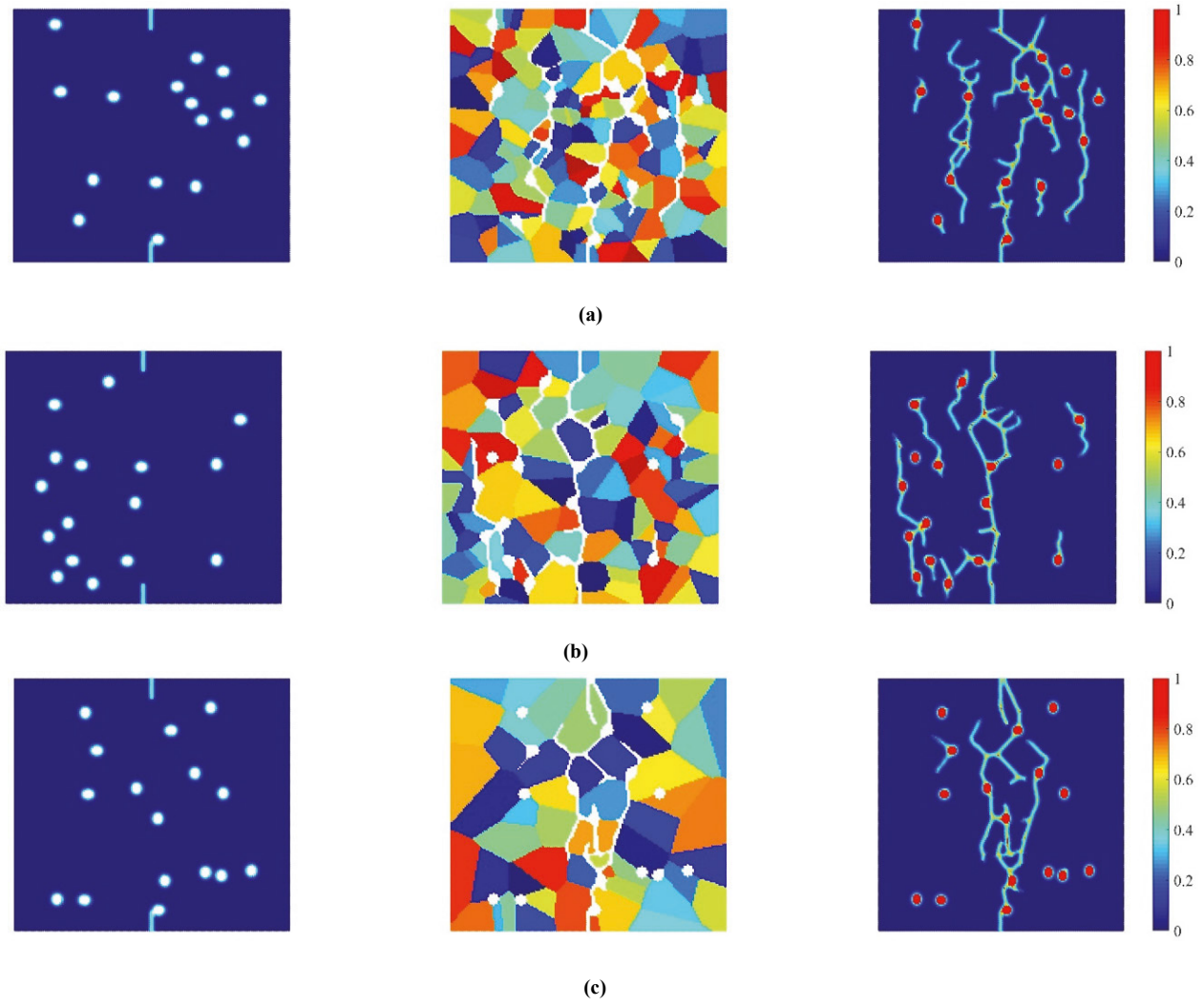

Fig. 8. Porosity distribution (left), crack distribution with grains (middle) and damage at 2 μs (right), (a) 150 grains, (b) 100 grains, (c) 50 grains

Finally, the GBC value is increased from 0.5 to 1. The remaining variables are kept the same. By doing so, the behaviour at the microscale becomes more identical to the macroscopic material. It is obvious that the behaviour of the main cracks is converted from intergranular pattern to transgranular pattern (Fig. 10).

In conclusion, the severity of the crack especially the newly created cracks are influenced by the number of grains and porosity. Concerning the influence of grain boundary strength, with the increase of GBC, the effect of porosity dramatically decreases and the fracture pattern in microscale becomes identical to the macroscale crack pattern.

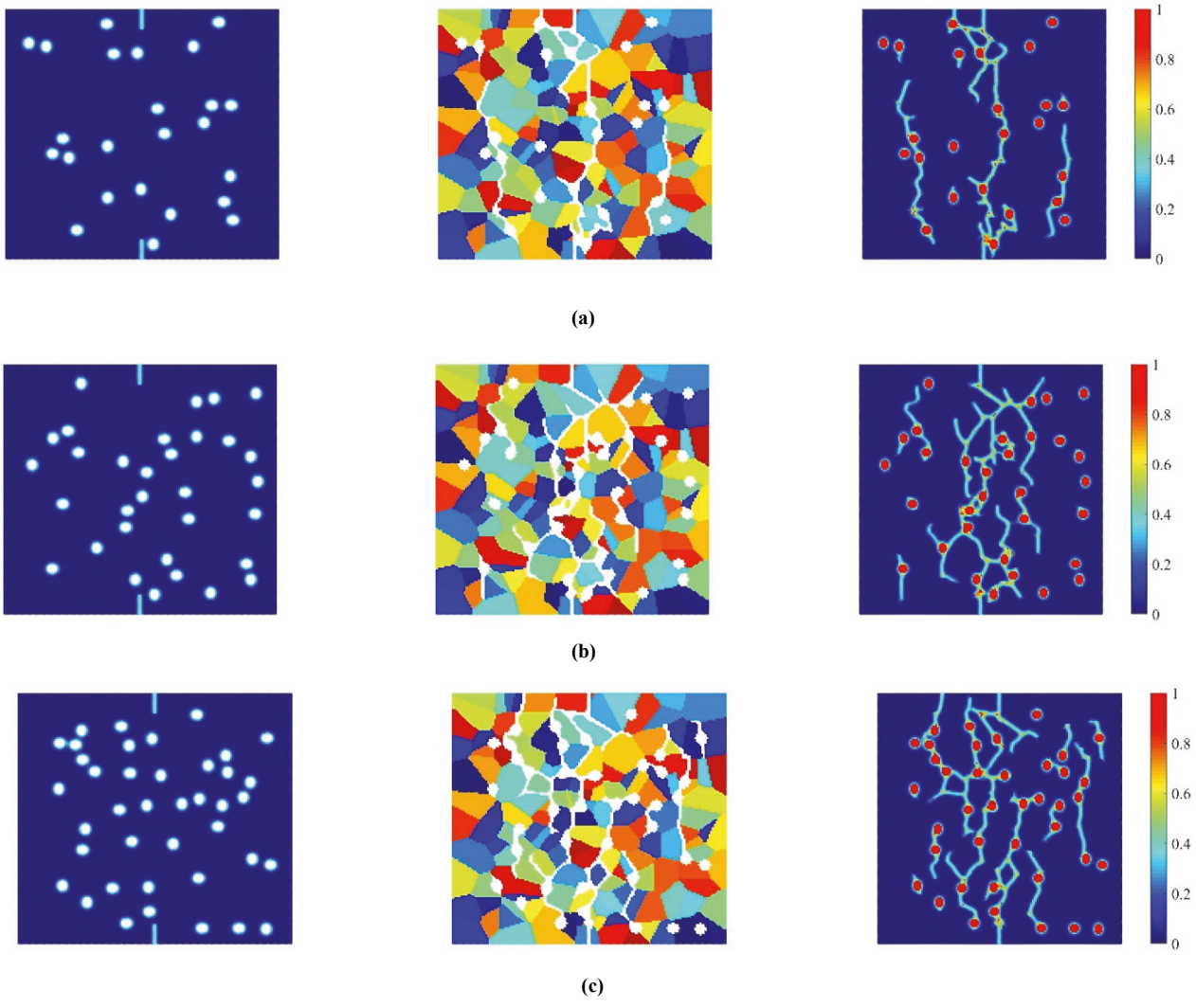

Fig. 9. Porosity distribution (left), crack distribution with grains (middle) and damage at 2 μs (right), (a) 3% porosity, (b) 4% porosity, (c) 5% porosity

4. Conclusions

In this study, the effect of porosity on intergranular brittle fracture was investigated by using peridynamics. Different number of cases were considered for different number of grains, different porosity ratios, different locations of pores and different grain boundary strengths. It was concluded that the severity of the crack especially the newly created cracks are influenced by the number of grains and porosity. Concerning the influence of grain boundary strength, with the increase of GBC, the effect of porosity dramatically decreases and the fracture pattern in microscale becomes identical to the macroscale crack pattern.

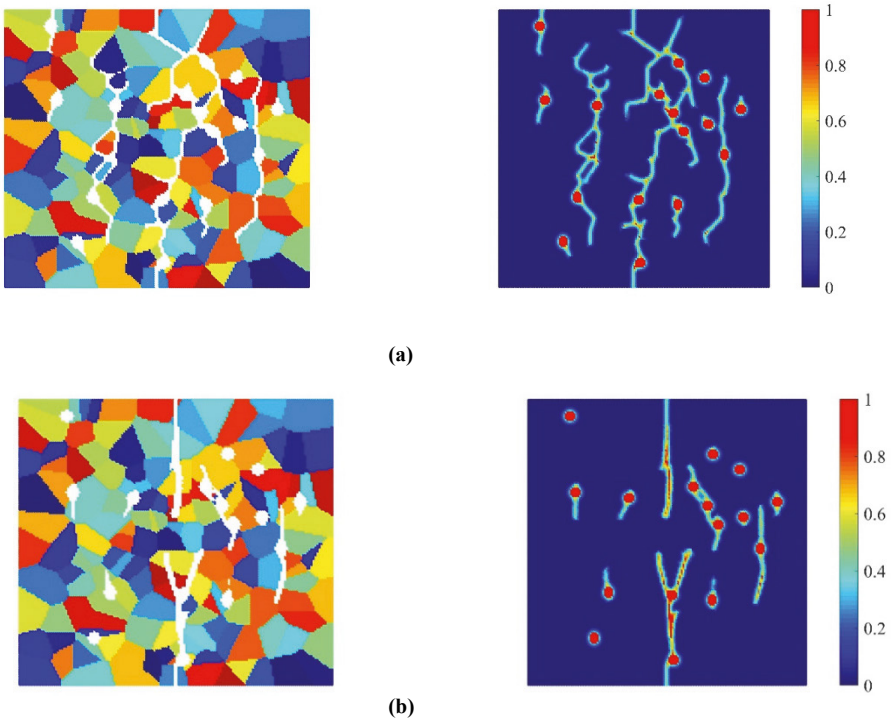

Fig. 10. Crack distribution with grains (left) and damage at 2 μs (right), (a) GBC = 0.5, (b) GBC = 1.0

References

Basoglu, M.F., Zerin, Z., Kefal, A., Oterkus, E., 2019. A computational model of peridynamic theory for deflecting behavior of crack propagation with micro-cracks. Computational Materials Science 162, 33–46.
Chakraborty, P., Zhang, Y., Tonks, M.R., 2016. Multi-scale modeling of microstructure dependent intergranular brittle fracture using a quantitative phase-field based method. Computational Materials Science 113, 38–52.
De Meo, D., Zhu, N., Oterkus, E., 2016. Peridynamic modeling of granular fracture in polycrystalline materials. Journal of Engineering Materials and Technology 138(4), 041008.
De Meo, D., Oterkus, E., 2017. Finite element implementation of a peridynamic pitting corrosion damage model. Ocean Engineering 135, 76–83.
De Meo, D., Russo, L., Oterkus, E., 2017. Modeling of the onset, propagation, and interaction of multiple cracks generated from corrosion pits by using peridynamics. Journal of Engineering Materials and Technology 139(4), 041001.
Diyaroglu, C., Oterkus, E., Oterkus, S., Madenci, E., 2015. Peridynamics for bending of beams and plates with transverse shear deformation. International Journal of Solids and Structures, 69, 152–168.
Diyaroglu, C., Oterkus, S., Oterkus, E., Madenci, E., 2017. Peridynamic modeling of diffusion by using finite-element analysis. IEEE Transactions on Components, Packaging and Manufacturing Technology 7(11), 1823–1831.
Diyaroglu, C., Oterkus, S., Oterkus, E., Madenci, E., Han, S., Hwang, Y., 2017. Peridynamic wetness approach for moisture concentration analysis in electronic packages. Microelectronics Reliability 70, 103–111.
Diyaroglu, C., Oterkus, E., Oterkus, S., 2019. An Euler–Bernoulli beam formulation in an ordinary state-based peridynamic framework. Mathematics and Mechanics of Solids 24(2), 361–376.
Imachi, M., Tanaka, S., Bui, T.Q., Oterkus, S., Oterkus, E., 2019. A computational approach based on ordinary state-based peridynamics with new transition bond for dynamic fracture analysis. Engineering Fracture Mechanics 206, 359–374.
Imachi, M., Tanaka, S., Ozdemir, M., Bui, T.Q., Oterkus, S., Oterkus, E., 2020. Dynamic crack arrest analysis by ordinary state-based peridynamics. International Journal of Fracture 221(2), pp.155–169.
Javili, A., Morasata, R., Oterkus, E., Oterkus, S., 2019. Peridynamics review. Mathematics and Mechanics of Solids 24(11), 3714-3739.
Kefal, A., Sohouli, A., Oterkus, E., Yildiz, M., Suleman, A., 2019. Topology optimization of cracked structures using peridynamics. Continuum Mechanics and Thermodynamics 31(6), 1645–1672.
Li, M., Lu, W., Oterkus, E., Oterkus, S., 2020. Thermally-induced fracture analysis of polycrystalline materials by using peridynamics. Engineering Analysis with Boundary Elements 117, 167–187.
Liu, X., He, X., Wang, J., Sun, L., Oterkus, E., 2018. An ordinary state-based peridynamic model for the fracture of zigzag graphene sheets. Proceedings of the Royal Society A: Mathematical, Physical and Engineering Sciences 474(2217), p.20180019.
Lu, W., Li, M., Vazic, B., Oterkus, S., Oterkus, E., Wang, Q., 2020. Peridynamic modelling of fracture in polycrystalline ice. Journal of Mechanics 36(2), 223–234.
Madenci, E., Oterkus, E., 2014. Peridynamic theory. Springer, New York, NY.

Oterkus, E., Barut, A., Madenci, E., 2010a. Damage growth prediction from loaded composite fastener holes by using peridynamic theory. In 51st AIAA/ASME/ASCE/AHS/ASC Structures, Structural Dynamics, and Materials Conference 18th AIAA/ASME/AHS Adaptive Structures Conference, Orlando, Florida, USA, p. 3026.
Oterkus, E., Guven, I. and Madenci, E., 2010b. Fatigue failure model with peridynamic theory. In 12th IEEE Intersociety Conference on Thermal and Thermomechanical Phenomena in Electronic Systems, Las Vegas, Nevada, USA, p. 1-6.
Oterkus, E., Madenci, E., 2012a. Peridynamics for failure prediction in composites. In 53rd AIAA/ASME/ASCE/AHS/ASC Structures, Structural Dynamics and Materials Conference 20th AIAA/ASME/AHS Adaptive Structures Conference, Honolulu, Hawaii, USA, p. 1692.
Oterkus, E., Madenci, E., 2012b. Peridynamic theory for damage initiation and growth in composite laminate. Key Engineering Materials 488, 355–358.
Oterkus, E., Guven, I., Madenci, E., 2012. Impact damage assessment by using peridynamic theory. Open Engineering 2(4), 523–531.
Oterkus, S., Madenci, E., Oterkus, E., Hwang, Y., Bae, J., Han, S., 2014, May. Hygro-thermo-mechanical analysis and failure prediction in electronic packages by using peridynamics. In 2014 IEEE 64th Electronic Components and Technology Conference (ECTC), Orlando, Florida, USA, p. 973-982.
Rimoli, J.J., 2009. A computational model for intergranular stress corrosion cracking. Doctoral dissertation, California Institute of Technology.
Silling, S.A., 2000. Reformulation of elasticity theory for discontinuities and long-range forces. Journal of the Mechanics and Physics of Solids 48(1), 175–209.
Vazic, B., Wang, H., Diyaroglu, C., Oterkus, S., Oterkus, E., 2017. Dynamic propagation of a macrocrack interacting with parallel small cracks. AIMS Materials Science 4(1), pp.118–136.
Vazic, B., Oterkus, E., Oterkus, S., 2020. Peridynamic model for a Mindlin plate resting on a Winkler elastic foundation. Journal of Peridynamics and Nonlocal Modeling, pp.1–10.
Wang, H., Oterkus, E., Oterkus, S., 2018. Predicting fracture evolution during lithiation process using peridynamics. Engineering Fracture Mechanics 192, 176–191.
Yang, Z., Oterkus, E., Nguyen, C.T., Oterkus, S., 2019. Implementation of peridynamic beam and plate formulations in finite element framework. Continuum Mechanics and Thermodynamics 31(1), 301–315.
Yang, Z., Vazic, B., Diyaroglu, C., Oterkus, E., Oterkus, S., 2020. A Kirchhoff plate formulation in a state-based peridynamic framework. Mathematics and Mechanics of Solids 25(3), 727–738.
Zhu, N., De Meo, D., Oterkus, E., 2016. Modelling of granular fracture in polycrystalline materials using ordinary state-based peridynamics. Materials 9(12), p.977.